Dopaminergic neurons of system x_c^--deficient mice are highly protected against 6-hydroxydopamine-induced toxicity

Ann Massie,*[,1] Anneleen Schallier,* Seong Woong Kim,[†] Ruani Fernando,[‡] Sho Kobayashi,[§] Heike Beck,[‖] Dimitri De Bundel,* Katia Vermoesen,* Shiro Bannai,[§] Ilse Smolders,* Marcus Conrad,[¶,2] Nikolaus Plesnila,[†] Hideyo Sato,[§] and Yvette Michotte*

*Department of Pharmaceutical Chemistry and Drug Analysis, Research Group Experimental Pharmacology, Vrije Universiteit Brussel, Brussels, Belgium; [†]Royal College of Surgeons in Ireland, Dublin, Ireland; [‡]Department of Medical Biochemistry and Biophysics, Karolinska Institutet, Stockholm, Sweden; [§]Department of Food and Applied Life Sciences, Faculty of Agriculture, Yamagata University, Tsuruoka, Yamagata, Japan; [‖]Walter Brendel Center of Experimental Medicine, Ludwig-Maximilians-University, Munich, Germany; and [¶]Helmholtz Center Munich, Institute of Clinical Molecular Biology and Tumor Genetics, Munich, Germany

ABSTRACT **Malfunctioning of system x_c^-, responsible for exchanging intracellular glutamate for extracellular cystine, can cause oxidative stress and excitotoxicity, both important phenomena in the pathogenesis of Parkinson's disease (PD). We used mice lacking xCT ($xCT^{-/-}$ mice), the specific subunit of system x_c^-, to investigate the involvement of this antiporter in PD. Although cystine that is imported *via* system x_c^- is reduced to cysteine, the rate-limiting substrate in the synthesis of glutathione, deletion of xCT did not result in decreased glutathione levels in striatum. Accordingly, no signs of increased oxidative stress could be observed in striatum or substantia nigra of $xCT^{-/-}$ mice. In sharp contrast to expectations, $xCT^{-/-}$ mice were less susceptible to 6-hydroxydopamine (6-OHDA)-induced neurodegeneration in the substantia nigra pars compacta compared to their age-matched wild-type littermates. This reduced sensitivity to a PD-inducing toxin might be related to the decrease of 70% in striatal extracellular glutamate levels that was observed in mice lacking xCT. The current data point toward system x_c^- as a possible target for the development of new pharmacotherapies for the treatment of PD and emphasize the need to continue the search for specific ligands for system x_c^-.—Massie, A., Schallier, A., Kim, S. W., Fernando, R., Kobayashi, S., Beck, H., De Bundel, D., Vermoesen, K., Bannai, S., Smolders, I., Conrad, M., Plesnila, N., Sato, H., Michotte, Y. Dopaminergic neurons of system x_c^--deficient mice are highly protected against 6-hydroxydopamine-induced toxicity. *FASEB J.* 25, 1359–1369 (2011). www.fasebj.org**

Key Words: xCT · glutathione · glutamate · Parkinson's disease

Oxidative stress and excitotoxicity are important mediators in the pathogenesis of neurodegenerative disorders. More particularly, in Parkinson's disease (PD), increased extracellular striatal glutamate levels and overactivity of the subthalamic nucleus (STN) contribute to neurodegeneration (1). Moreover, glutathione, the most important antioxidant in the brain, has an important and early role in the pathogenesis of PD. The severity of the disease correlates with the loss of glutathione, and the decrease in nigral glutathione precedes any other alteration in biochemical marker (2).

System x_c^- or the cystine/glutamate antiporter (with xCT as specific subunit) is an Na^+-independent heteroexchanger importing 1 cystine molecule into the cell in exchange for 1 glutamate molecule. Cystine is intracellularly reduced to cysteine, the rate-limiting substrate in the synthesis of glutathione (3). Baker *et al.* (4) reported that in rat nucleus accumbens, system x_c^- is the major source of extracellular glutamate. The involvement of system x_c^- in the pathogenesis of PD can thus be dual: increased activity could protect the brain against oxidative stress, while, at the same time, the increased release of glutamate could lead to excitotoxicity. Yet, until now, *in vivo* evidence for the true involvement of system x_c^- in neurodegenerative diseases has been lacking. Whereas overexpression of xCT has been described as a reason for neurodegeneration in specific conditions, *i.e.*, in the vicinity of tumors (5), surrounding amyloid-β plaques (6) and in *Drosophila melanogaster* (7), accumulating *in vitro* evidence points

[1] Correspondence: Department of Pharmaceutical Chemistry and Drug Analysis, Vrije Universiteit Brussel, Laarbeeklaan 103, 1090 Brussels, Belgium. E-mail: amassie@vub.ac.be

[2] Current address: German Center for Neurodegenerative Diseases and Helmholtz Center Munich, Institute of Developmental Genetics, Ingolstädter Landstrasse 1, 85764 Munich-Neuherberg, Germany.

doi: 10.1096/fj.10-177212

toward system x_c^- as a possible neuroprotective drug target (8). Recently, we described an ipsilateral up-regulation of xCT in striatum of the hemi-Parkinson rat (9). Possibly, this up-regulation is a compensatory reaction of the brain in response to increased oxidative stress. Yet, it might also cause increased extracellular glutamate concentrations, as described in the striatum of this rat model (10, 11). To unveil whether this up-regulation of xCT in the parkinsonian striatum is protective by providing more cysteine to cells or rather deteriorates the situation by increasing extracellular glutamate, we used transgenic mice with a deletion of the xCT gene, and thus lacking functional system x_c^- (12). We illustrated that these mice do not show any signs of increased oxidative stress in the striatum. Surprisingly, although the striatal dopamine (DA) loss following 6-OHDA injection in the $xCT^{-/-}$ mice was equal to $xCT^{+/+}$ mice, dopaminergic neurons in the substantia nigra pars compacta (SNc) of $xCT^{-/-}$ mice were protected against 6-OHDA-induced toxicity. Although we were unable to identify any effect of the loss of glial cystine import, the loss of glutamate release *via* system x_c^- significantly reduced striatal extracellular glutamate levels.

In summary, the loss of xCT expression could not block primary 6-OHDA toxicity, but it did protect neurons of the SNc from degeneration. This is the first report pointing toward system x_c^- as a novel target for the development of pharmacotherapies for PD.

MATERIALS AND METHODS

Animals

Studies were performed according to national guidelines on animal experimentation and were approved by the Ethical Committee for Animal Experimentation of the Faculty of Medicine and Pharmacy of the Vrije Universiteit Brussel.

$xCT^{-/-}$ mice used in this study were descendants of the strain described in a previous study (12). The mice were outbred to wild-type C57BL/6 mice for ≥12 generations before use. For this study, both young (12–16 wk) and old (12–18 mo) $xCT^{-/-}$ mice were used. Age-matched wild-type littermates served as controls. Genotypes were confirmed by PCR of tail DNA, using the REDExtract-N-Amp Tissue PCR kit (Sigma-Aldrich, St. Louis, MO, USA) and the following primers: 5′-GATGCCCTTCAGCTCGATGCGGTTCACCAG-3′ (GFPR3); 5′-CAGAGCAGCCCTAAGGCACTTTCC-3′ (mxCT5′flankF6); and 5′-CCGATGACGCTGCCGATGATGATGG-3′ [mxCT(Dr4)R8].

Striatal 6-OHDA lesioning

Mice were anesthetized with a mixture of ketamine:xylazine (10:10 mg/kg, i.p.) and placed in a stereotactic frame. The skull was exposed, and a small hole was made through the skull at the appropriate location. A 6-OHDA solution [containing 4 μg/μl 6-OHDA (Sigma-Aldrich) in 0.01% ascorbic acid, pH 5.0] was stereotactically injected into the striatum at coordinates L −1.8, AP 0.4, DV 3.5, relative to bregma, according to the atlas of Paxinos and Franklin (13). A total volume of 1.5 μl 6-OHDA solution was injected at a flow rate of 0.5 μl/min. The syringe was left in place for 5 min and then slowly removed over a 1- to 2-min time period. Sham-operated mice were injected with vehicle only. The skin was sutured, and the mice received 4 mg/kg i.p. ketofen (Merial, Brussels, Belgium) to provide postoperative analgesia. Mice were sacrificed on d 3 and 10 after 6-OHDA injection. At d 3, a maximal DA loss in ipsilateral striatum was already observed (see Fig. 3*A*, *B*), whereas neurodegeneration was not very pronounced in the SNc of $xCT^{+/+}$ mice and absent in $xCT^{-/-}$ mice (see Fig. 4*E*, *F*). Therefore, we additionally examined brains at d 10 postlesion, when average neurodegeneration reached 25% in wild-type mice.

HPLC analysis of DA and DOPAC

Mice were killed by cervical dislocation. Brains were rapidly removed, and the caudal part was postfixed for 3 d in freshly prepared 4% paraformaldehyde. From the rostral part of the brain, striata were isolated and weighed, before homogenization in 400 μl antioxidant solution (0.05M HCl, 0.5% $Na_2S_2O_5$, and 0.05% Na_2EDTA) containing 40 ng 3,4-dihydroxybenzylamine (DHBA) as an internal standard. The homogenate was centrifuged for 10 min at 10000 *g*, and the supernatants were stored at −80°C. The supernatant was diluted 1:5 in 0.5 M acetic acid and analyzed for its DA and DOPAC content on a narrow-bore (column C18 5 μm, 150×2.1 mm; Unijet; Bioanalytical Systems, West Lafayette, IN, USA) liquid chromatography system with an electrochemical detector (Intro; Antec, Leiden, The Netherlands). The mobile phase consisted of 0.1 M Na-acetate, 20 mM citric acid, 1 mM Na-octanesulfonate, 1 mM dibutylamine, and 0.1 M Na_2EDTA, adjusted to pH 3.8. Methanol was added as an organic modifier (3% v/v). As a standard, a mixture of DHBA (1 ng/100 μl), DA (5 ng/100 μl) and DOPAC (2 ng/100 μl) was used. Statistical analysis of the data was performed using a 2-way ANOVA followed by Bonferroni *post hoc* test ($\alpha=0.05$).

Immunohistochemistry

For the 6-OHDA-lesioned mice in which the striatum was used for HPLC analysis, 40-μm vibratome sections were made of the postfixed caudal part of the brain. Mice in which the brain was only used for immunohistochemistry were transcardially perfused with a physiological solution followed by freshly depolymerized 4% paraformaldehyde (Sigma-Aldrich) in 0.15 M PBS (pH 7.42). Next, brains were removed and postfixed in the same fixative overnight, rinsed in tap water for 24 h, and stored in 0.015 M PBS at 4°C. Free-floating 40-μm frontal sections were made with a vibratome and stored in serial order in 0.015 M PBS at 4°C.

All rinsing steps and incubations of the staining procedure were performed in Tris-saline (0.01 M, 0.1% Triton X-100, pH 7.4; Sigma-Aldrich) at room temperature and under gentle agitation. The sections underwent a permeabilizing treatment consisting of incubation in 0.1% trypsin (Fluka, Buchs, Switzerland) for 1 h at 37°C. An incubation of 30 min in 3% H_2O_2 and a blocking step with normal goat serum (diluted 1:5, 45 min; Millipore, Temecula, CA, USA) preceded overnight incubation with the immunoaffinity-purified polyclonal tyrosine hydroxylase (TH; 1:2000; Millipore), 4-hydroxy-2-nonenal (HNE; 1:500; Alpha Diagnostic, San Antonio, TX, USA), nitrotyrosine (NT; 1:100, Millipore), or heme oxygenase-1 (HO-1; 1:10,000; Stressgen, Ann Arbor, MI, USA) antibodies raised in rabbit. The next day, sections were processed by the avidin-biotin method using a Vectastain ABC kit (Vector Laboratories, Burlingame, CA, USA), and immunoreactivity was visualized, after a final rinsing step with acetate buffer, using the glucose oxidase-diaminobenzidine-nickel method (14).

As for confocal microscopy, sections were washed in PBS, and nonspecific interactions were blocked by 1 h incubation in 5% normal donkey serum (NDS), 2% BSA, and 0.3% Triton X-100 in PBS. Sections were incubated with rabbit anti-GFAP (DakoCytomation, Glostrup, Denmark; 1:1000) diluted in 0.3% Triton X-100, 0.1% BSA, and 1% NDS in PBS overnight at 4°C. GFAP was visualized with donkey Alexa IgG 555 (Invitrogen, Merelbeke, Belgium; 1:800) in 2% BSA in PBS.

Photomicrographs were made of the stained sections, and cell counts were performed using ImageJ software (U.S. National Institutes of Health, Bethesda, MD, USA). Total numbers of TH^+ profiles in the SNc were counted in 6 serial sections with an interval of 120 μm (every 3 sections, 1 section was stained). The total number of TH^+ profiles in the 6 consecutive sections was multiplied by 3 (15). The number of $GFAP^+$ cells in the striatum was evaluated on 6 consecutive 40-μm slices between 1.10 and 0.38 mm rostral from bregma.

Wilcoxon test for matched pairs was used to compare the number of TH^+ profiles between ipsilateral and contralateral SNc of a 6-OHDA-injected mouse or sham-injected mouse of a given condition. Statistical comparison of the percentage loss of TH^+ profiles between $xCT^{+/+}$ and $xCT^{-/-}$ cells, as well as comparison of the number of $GFAP^+$ cells between young and old $xCT^{+/+}$ and $xCT^{-/-}$ mice, was accomplished using a 2-way ANOVA followed by Bonferroni's *post hoc* test.

Glutathione assay

Following cervical dislocation, the striatum was quickly dissected and homogenized in an ice-cold buffer containing 2 mM EDTA and 20 mM Tris at pH 7.4. Homogenates were centrifuged for 15 min at 10,000 *g*, and protein content of the supernatant was determined using a Quant-iT Protein Assay Kit (Invitrogen). The glutathione content of the supernatant was subsequently analyzed using a QuantiChrom Glutathione Assay Kit (BioAssay Systems, Hayward, CA, USA), according to the manufacturer's instructions. The method essentially consists of a deproteination step followed by a colorimetric reaction of glutathione with 5,5′-dithiobis(2-nitrobenzoic acid), yielding a yellow reaction product. Optical density at 415 nm was measured on a plate reader.

Statistical analysis of glutathione levels in young and old $xCT^{+/+}$ compared to $xCT^{-/-}$ mice was performed using a 2-way ANOVA followed by Bonferroni's *post hoc* test.

Western blot analysis

Following cervical dislocation, brains were rapidly removed and snap-frozen. Striatal tissue was isolated from 100-μm cryosections. Protein extraction and Western blot analysis was performed as described previously (16). The primary antibodies included rabbit antibody to xCT (9); guinea pig antibody to VGLUT1 (1:2000; Millipore); mouse antibody to VGLUT2 (1:5000; Millipore); rabbit antibody to VGLUT3 (1:5000; Covalab, Villeurbanne, France); rabbit antibody to GLT-1 (1:30,000; ref. 17); rabbit antibody to GLAST (1:4000; ref. 18); rabbit antibody to EAAC1 (1:1000; Alpha Diagnostic); rabbit antibody to TH (1:4000; Millipore); mouse antibody to synaptophysine (1:5000; Stressgen); rabbit antibody to GAPDH (1:5000; Santa Cruz Biotechnology, Santa Cruz, CA, USA); and mouse antibody to GAPDH (1:15000; Millipore). The antibodies were visualized by chemiluminescence (ECL Plus kit; GE Healthcare, Roosendaal, The Netherlands) after incubation with horseradish peroxidase-conjugated antibody to rabbit, mouse (DakoCytomation) or guinea pig IgG (Millipore). Optical density (OD) of the protein bands was measured using ImageJ and normalized to the density of GAPDH, visualized on the same membrane. An arbitrary chosen $xCT^{+/+}$ sample was set as a reference (100%), and the OD of all other samples was calculated relative to this reference. Statistical analysis was performed using a Mann-Whitney *U* test.

Microdialysis and dialysate glutamate determination

At 24 h before sampling, vertical microdialysis probes (0.24 mm outer diameter, 2-mm membrane length; CMA; Microdialysis AB, Solna, Sweden) were stereotactically implanted in the left striatum of mice under anesthesia. The probe was implanted in the striatum at coordinates L 2.0, AP 0.6, DV 2, relative to bregma, according to the atlas of Paxinos and Franklin (13). The external portions of the probes were fixed to the skull with dental cement. Dialysis probes were perfused with Ringer solution (147 mM NaCl, 2.3 mM $CaCl_2$, and 4.0 mM KCl; pH 7.0) at a rate of 2 μl/min. The microdialysate (20 μl) was collected every 10 min.

For glutamate analysis of the microdialysates, we used a reversed-phase narrow-bore assay with gradient elution and fluorescence detection. The dialysate (15 μl) was automatically derivatized with *o*-phtalaldehyde in the presence of β-mercaptoethanol at 4°C by a cooled (832 temperature regulator; Gilson, Villiers Le Bel, France) 231 XL sampling injector (Gilson). This 1-step precolumn derivatization preceded the injection of 10 μl of the sample on a C18 narrow-bore column (5-μm particle size, 250 × 2 mm; Capcell Pak MG, Shiseido, Japan). The samples were eluted by a Dionex P680 HPLC pump (Dionex Benelux, Amsterdam, The Netherlands) with the previously described mobile phases and gradient program (19). Detection was performed with a RF10A XL fluorescence detector (Shimadzu, Kyoto, Japan); the limit of detection of this narrow-bore assay was 30 nM. All microdialysis data are expressed as mean ± SE glutamate level (μM). Statistical analysis was performed using a Mann-Whitney *U* test.

Total striatal glutamate content

Following cervical dislocation, brains were rapidly removed. Striatum was dissected, weighed, homogenized in 500 μl 0.1 N HCl_4, and spun for 5 min at 10,000 *g*. An equal volume of 0.1 N NaOH was added to the supernatants and vortexed. Samples were diluted 25× in Ringer's solution, and glutamate content was determined as described above for dialysates. Data are expressed as mean ± SE glutamate level (ng/g wet tissue). Statistical analysis was performed using a Mann-Whitney *U* test.

Cystine uptake and intracellular glutathione content in C6 glioma treated with 6-OHDA

C6 glioma cells were plated (200,000 cells/35-mm culture dish) and cultured for 24 h in Dulbecco's modified Eagle's medium supplemented with 10% FBS at 37°C in 5% CO_2 and 95% air. In a first experiment, 6-OHDA was added at a concentration of 10, 20, or 50 μM, and cells were cultured for another 24 h. Cystine uptake was measured as described in Sato *et al.* (12). The uptake solution was 10 mM PBS (137 mM NaCl and 3 mM KCl), pH 7.4, containing 0.01% $CaCl_2$, 0.01% $MgCl_2 \cdot 6\ H_2O$, 0.1% glucose, and L-[^{14}C]cystine (0.05 mM and 7.4 kBq/ml). Total glutathione in the cells was measured by the enzymatic method described previously (12), which is based on the catalytic action of glutathione reductase system. In a second series of experiments, the cells were cultured with 20 μM 6-OHDA for 24 h, and then cystine uptake was measured in the presence or absence of Na^+ (Na^+ replaced

by choline), and with 2.5 mM glutamate or 2.5 mM homocysteic acid (HoA) added to the uptake solution. Finally, intracellular glutathione levels were measured after cells were incubated with 20 μM 6-OHDA for 24 h in the presence of an excess amount of glutamate (5 and 10 mM). Statistical analysis was performed using a 1- or 2-way ANOVA followed by Bonferroni's *post hoc* test.

RESULTS

Oxidative stress-related markers in striatum and substantia nigra of xCT-knockout mice

Expression of oxidative stress-related markers HNE, NT, and HO-1 revealed no genotype-related differences. In general, striatal and nigral expression were very faint in both young and old mice (data not shown).

Effect of aging on striatal glutathione levels and gliosis

The density of $GFAP^+$ cells in the striatum was similar between $xCT^{-/-}$ mice and their age-matched wild-type littermates (young $xCT^{+/+}$ *vs.* $xCT^{-/-}$: 32.33±3.54 *vs.* 31.35±0.94 cells/mm^2; old $xCT^{+/+}$ *vs.* $xCT^{-/-}$: 60.98±2.59 *vs.* 57.76±2.76 cells/mm^2; 2-way ANOVA followed by Bonferroni's *post hoc* test, $F_{1,19}$=3.63, n.s.). Yet, there was a clear age-dependent effect on gliosis in the striatum in both genotypes (2-way ANOVA followed by Bonferroni's *post hoc* test, $F_{1,19}$=623.4, P<0.0001; **Fig. 1*A–E***).

Striatal glutathione content decreased age dependently in both genotypes (2-way ANOVA with Bonferroni's *post hoc* test, $F_{1,20}$=93.32, P<0.0001). However, we could not observe any genotype-related effect (young $xCT^{+/+}$ *vs.* $xCT^{-/-}$: 71.8±2.4 *vs.* 69.5±1.8 nmol/mg protein; old $xCT^{+/+}$ *vs.* $xCT^{-/-}$: 49.1±2.2 *vs.* 48.9±2.5 nmol/mg protein; 2-way ANOVA with Bonferroni's *post hoc* test, $F_{1,20}$=0.31, n.s.; Fig. 1*F*).

Nigrostriatal dopaminergic pathway in xCT-knockout mice

No difference could be detected in striatal DA content between young and old $xCT^{-/-}$ mice (20,303±1716 and 21680±1072 ng/g wet tissue, respectively) and their age-matched wild-type littermates (21,683±1072 and 23,260±1197 ng/g wet tissue, respectively; 2-way ANOVA with Bonferroni's *post hoc* test, $F_{1,26}$=1.10, n.s.; **Fig. 2*A***). Also, the striatal DOPAC/DA ratio was independent of genotype in both young ($xCT^{+/+}$ *vs.* $xCT^{-/-}$: 0.055±0.003 *vs.* 0.056±0.003) and old mice ($xCT^{+/+}$ *vs.* $xCT^{-/-}$: 0.049±0.002 *vs.* 0.050±0.002; 2-way ANOVA with Bonferroni's *post hoc* test, $F_{1,46}$=0.17, n.s.). Yet, there was a significant decrease in DOPAC/DA ratio with age in both genotypes (2-way ANOVA with Bonferroni's *post hoc* test, $F_{1,46}$=5.97, P=0.018; Fig. 2*B*). Moreover, we could not detect any difference in number of TH^+ profiles in the SNc of 18 consecutive 40-μm sections between $xCT^{-/-}$ (young and old: 1693±29 and 1787±64 profiles) and $xCT^{+/+}$ mice (young and old: 1758±79 and 1818±29 profiles). In addition, no effect of aging was detectable (2-way ANOVA with Bonferroni's *post hoc* test, $F_{1,60}$=0.71, n.s.; Fig. 2*C*).

Striatal DA loss after 6-OHDA lesioning

At 3 d following unilateral striatal 6-OHDA injection, both young $xCT^{-/-}$ mice and their wild-type littermates showed a striatal DA loss of ~50% ($xCT^{-/-}$ *vs.* $xCT^{+/+}$: 51.8±3.0 *vs.* 48.8±6.4%). Similarly, at 10 d postlesion, there was no difference in striatal DA loss between the genotypes ($xCT^{-/-}$ *vs.* $xCT^{+/+}$: 42.9±6.5 *vs.* 44.7±7.1%; 2-way ANOVA with Bonferroni's *post hoc* test, $F_{1,43}$=4, n.s.; **Fig. 3*A***). In addition, also in the old mice, striatal loss of DA between $xCT^{-/-}$ mice and their wild-type littermates was similar at d 3 (57.2±7.8

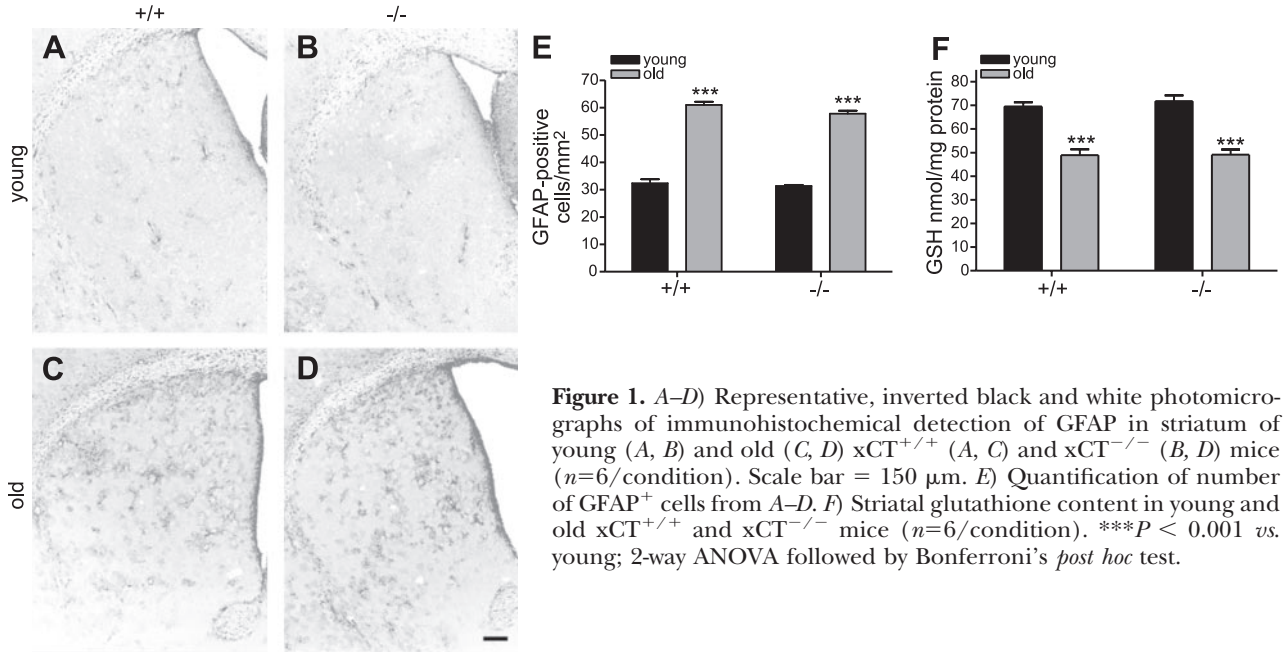

Figure 1. *A–D*) Representative, inverted black and white photomicrographs of immunohistochemical detection of GFAP in striatum of young (*A*, *B*) and old (*C*, *D*) $xCT^{+/+}$ (*A*, *C*) and $xCT^{-/-}$ (*B*, *D*) mice (n=6/condition). Scale bar = 150 μm. *E*) Quantification of number of $GFAP^+$ cells from *A–D*. *F*) Striatal glutathione content in young and old $xCT^{+/+}$ and $xCT^{-/-}$ mice (n=6/condition). ***P < 0.001 *vs.* young; 2-way ANOVA followed by Bonferroni's *post hoc* test.

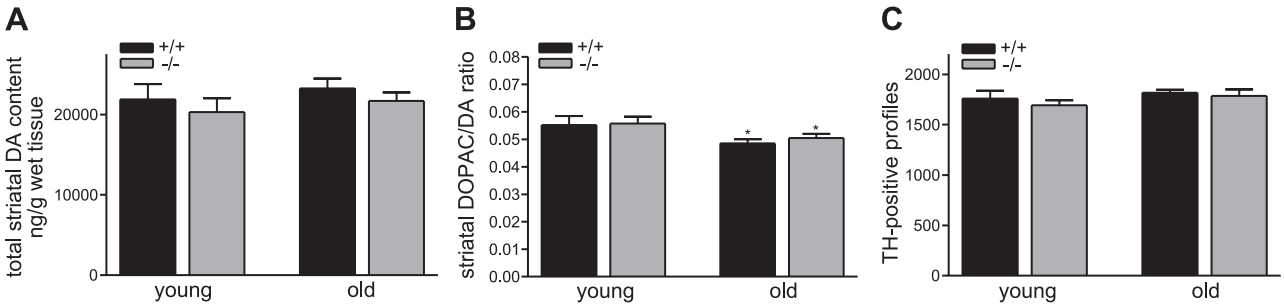

Figure 2. Total striatal DA content (*A*; n=6–9/condition), striatal DOPAC/DA ratio (*B*; n=10–16/condition) and number of TH^+ profiles in SNc (*C*; n=14–18/condition) of young and old $xCT^{+/+}$ and $xCT^{-/-}$ mice. *$P < 0.05$ *vs.* young; 2-way ANOVA followed by Bonferroni's *post hoc* test.

and 66.0±6.3%, respectively) and d 10 postlesion (45.5±7.6 and 43.3±8.8%, respectively; 2 -way ANOVA with Bonferroni's *post hoc* test, $F_{1,37}$=0.37, n.s.; Fig. 3*B*). DOPAC/DA ratio increased in the ipsilateral compared to the contralateral striatum in both genotypes and in both age groups at 3 d postlesion (young and old $xCT^{+/+}$: 136.7±4.0 and 161.7±24.3%; young and old $xCT^{-/-}$: 142.3±11.3 and 158.9±8.2%), whereas at 10 d postlesion, it returned to normal levels in all 4 experimental groups (young and old $xCT^{+/+}$: 117.5±5.7 and 110.5±6.4%; young and old $xCT^{-/-}$: 112.3±9.6 and 120.9±5.5%). No significant difference could be observed in DOPAC/DA ratio (2-way ANOVA with Bonferroni's *post hoc* test; young mice: $F_{1,43}$=0.08, n.s.; old mice: $F_{1,32}$=0.17, n.s.; Fig. 3*C, D*).

$xCT^{-/-}$ mice are highly protected against nigral neurodegeneration

Significant neurodegeneration (*i.e.*, loss of TH^+ neurons) could be observed in the ipsilateral SNc compared to the contralateral SNc at d 3 and 10 (Wilcoxon, P=0.03 and P=0.02, respectively) following unilateral

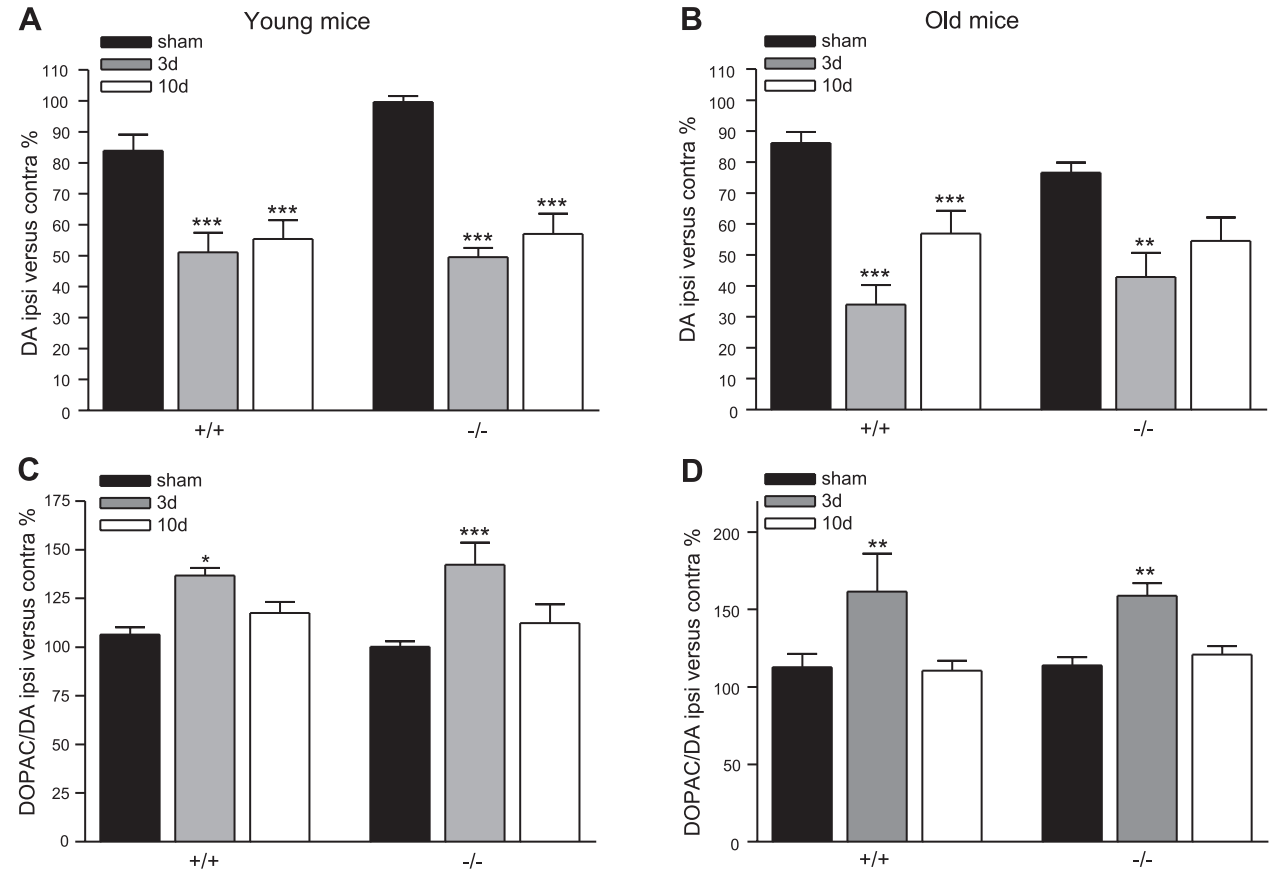

Figure 3. DA levels (*A, B*) and DOPAC/DA ratio (*C, D*) in ipsilateral striatum relative to contralateral striatum at 3 and 10 d postlesion in young (*A, C;* n=7–10/condition) and old (*B, D;* n=6–10/condition) $xCT^{+/+}$ and $xCT^{-/-}$ mice. *$P < 0.05$, **$P < 0.01$, ***$P < 0.001$ *vs.* sham treatment; 2-way ANOVA followed by Bonferroni's *post hoc* test.

injection of 6-OHDA into the striatum of young wild-type mice. In contrast, no significant loss of dopaminergic neurons in the SNc was detectable in xCT$^{-/-}$ mice at either d 3 or 10 postlesion (Wilcoxon, n.s.; **Fig. 4*E***). Studying old mice, significant neurodegeneration could only be observed in the ipsilateral SNc of xCT$^{+/+}$ mice (Wilcoxon, 3 d: P=0.03; 10 d: P=0.03), whereas xCT$^{-/-}$ mice are highly protected against neurodegeneration (Wilcoxon, n.s.; Fig. 4*A–D, F*). Comparing the percentage loss of neurons between xCT$^{+/+}$ mice and xCT$^{-/-}$ mice revealed a statistically significant genotype-dependent difference at both survival times in both young mice (xCT$^{+/+}$ and xCT$^{-/-}$, 3 d: 13.0±3.2 and −0.4±3.1%; 10 d: 24.0±1.4 and 7.4±2.1%; 2-way ANOVA with Bonferroni's *post hoc* test, $F_{1,36}$=12.55, P=0.0011) and old mice (xCT$^{+/+}$ and xCT$^{-/-}$, 3 d: 24.7±3.9 and 1.0±2.9%; 10 d: 24.0±4.4 and 3.8±3.3%; 2-way ANOVA with Bonferroni's *post hoc* test, $F_{1,29}$=19.23, P=0.0001; Fig. 4*G, H*).

No difference in the expression of oxidative stress-related markers in striatum and substantia nigra between wild-type and xCT$^{-/-}$ mice

Injection of 6-OHDA, or even vehicle alone, induced a strong up-regulation of striatal HO-1 expression in all 4 experimental groups. In sham-injected mice, this up-regulation was seen in the close vicinity of the needle track, whereas in 6-OHDA-lesioned mice, this up-regulation was apparent throughout a large part of striatum (**Fig. 5*A*, *B***). In addition, a slight and local up-regulation of both HNE and NT expression was observed at the site of 6-OHDA injection (Fig. 5*C, D*) in all 4 experimental groups. Also in the substantia nigra, we could not observe any effect of genotype on oxidative stress-related marker expression after 6-OHDA injection into the striatum. HNE and NT did not show any up-regulation in neurons of the SNc in 6-OHDA-injected animals compared to contralateral SNc or sham-injected mice (data not shown). HO-1 up-regulation could be detected in some neurons of the ipsilateral SNc of xCT$^{-/-}$ (Fig. 5*F*), as well as xCT$^{+/+}$ mice (data not shown, identical to xCT$^{-/-}$ mice), contrary to neurons of the contralateral SNc (Fig. 5*E*).

Strongly diminished extracellular glutamate levels in striatum of xCT-knockout mice

Extracellular glutamate levels were significantly decreased in the striatum of the xCT$^{-/-}$ mice compared to wild-type mice (0.14±0.04 and 0.48±0.12 μM, respectively; Mann-Whitney U=7.0, P=0.014; **Fig. 6*A***). Total striatal glutamate content, as measured in homogenates, was unaffected (xCT$^{+/+}$ and xCT$^{-/-}$: 1097.92±119.47 and 1145.52±128.80 μg/g wet tissue; U=16.0, P=0.82; Fig. 6*B*).

We examined striatal homogenates of young xCT$^{-/-}$ and xCT$^{+/+}$ mice by semiquantitative Western blotting to evaluate possible compensatory changes in expression levels of other glutamate transporters as a result of xCT gene deletion. None of the other glutamate transporters showed compensatory changes in striatal expression level in the

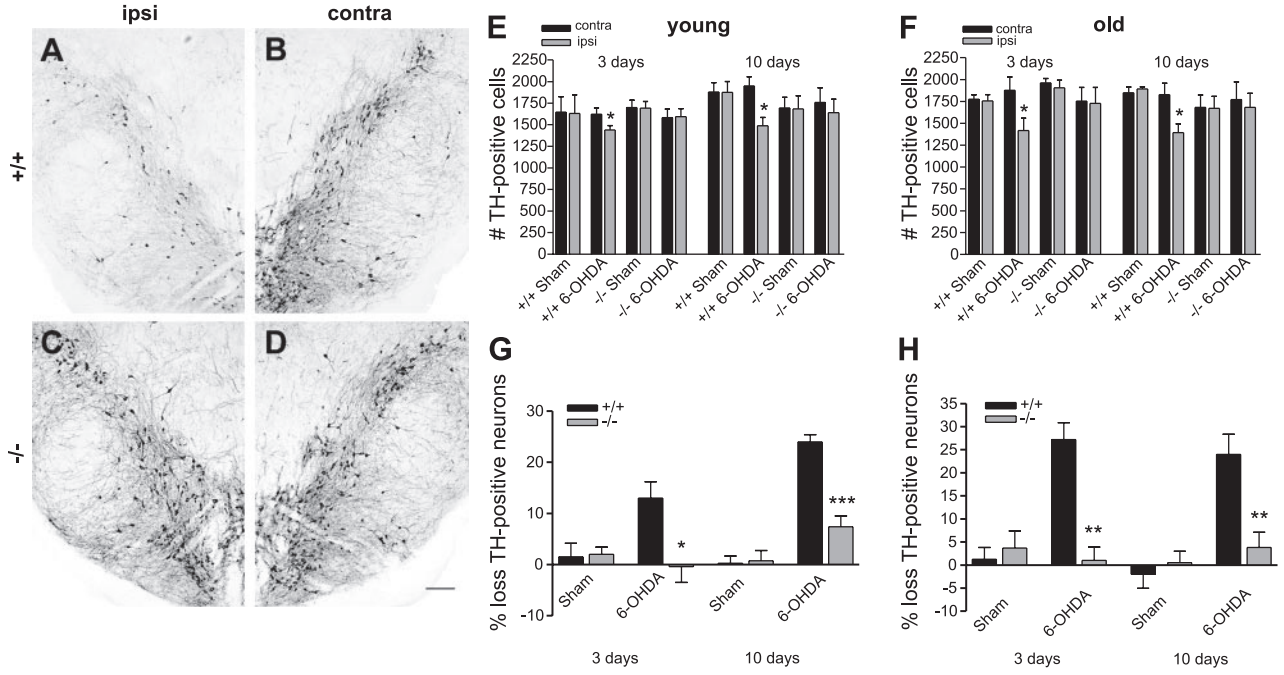

Figure 4. *A–D*) Representative example of TH staining in ipsilateral (ipsi; *A, C*) and contralateral (contra) SNc (*B, D*) of old xCT$^{+/+}$ (*A, B*) and xCT$^{-/-}$ (*C, D*) mice at d 3 postlesion. Scale bar = 100 μm. *E–H*) Number of TH$^+$ profiles in ipsilateral and contralateral SNc (*E, F*) and percentage loss of TH$^+$ profiles in ipsilateral compared to contralateral SNc (*G, H*) at 3 and 10 d after injecting 6-OHDA into the left striatum of young (*E, G*) and old mice (*F, H*; n=6 or 7/condition; n=4 or 5 for sham groups). *P < 0.05, **P < 0.01, ***P < 0.001 *vs.* xCT$^{+/+}$ (*G, H;* 2-way ANOVA followed by Bonferroni's *post hoc* test) or contra (*E, F;* Wilcoxon test).

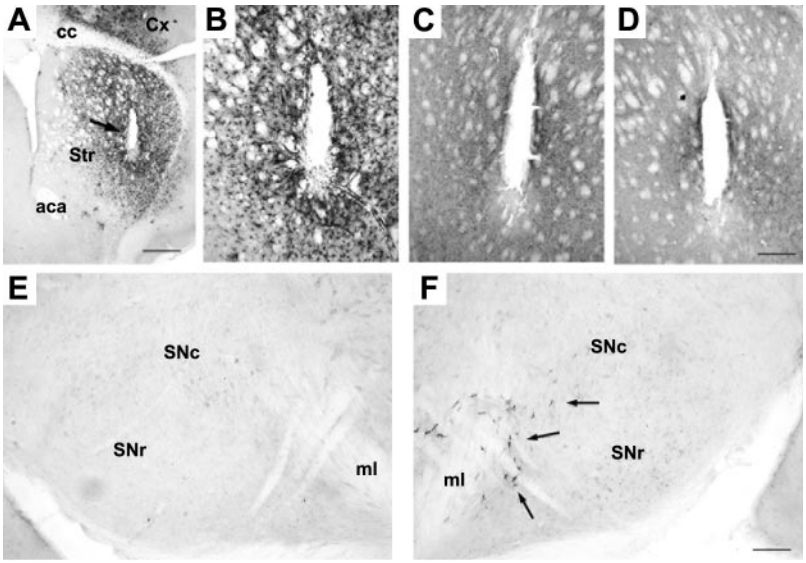

Figure 5. Representative photomicrograph of immunohistochemical staining for HO-1 (*A*, *B*, *E*, *F*), HNE (*C*), and NT (*D*) on ipsilateral striatum (*A–D*; Str) and substantia nigra (*E*, *F*; SN) 3 d after 6-OHDA injection into the striatum of an old $xCT^{-/-}$ mouse (n=6/condition). *A*) Strong increase in HO-1-immunoreactivity in the vicinity of the needle track (arrow) and injection site in the striatum. *B*) Magnified view of detail in panel *A*. *C, D*) Local increase of HNE (*C*) and NT (*D*) immunoreactivity at the injection site. *E, F*) HO-1-immunoreactivity in contralateral (*E*) and ipsilateral (*F*) SN. Arrows indicate scarce immunoreactive neurons in the SNc (*F*). Scale bars = 500 μm (A); 200 μm (*B–D*); 100 μm (*E, F*). aca, anterior commissure, anterior; cc, corpus callosum; Cx, cortex; SNr, substantia nigra pars reticulate; ml, medial lemniscus.

3-mo-old $xCT^{-/-}$ mice compared to their wild-type littermates [*i.e.* ($xCT^{+/+}$ *vs.* $xCT^{-/-}$; Mann-Whitney *U*), GLAST (100.3±18.5 *vs.* 119.4±16.0; U=9.0, n.s.), GLT-1 (99.6±25.8 *vs.* 97.4±15.2%; U=10.0, n.s.), EAAC1 (100.0±16.7 *vs.*105.8±18.8%; U=13, n.s.), VGLUT1 (100.4±19.6 *vs.* 117.1±19.3%; U=11.0, n.s.), VGLUT2 (99.7±11.1 *vs.* 109.8±10.8%; U=11.0, n.s.) or VGLUT3 (99.9±12.2 *vs.* 91.7±14.8%; U=6.0, n.s.); Fig. 6*C, D*]. Also, synaptophysin, a marker for presynaptic terminals, remained unchanged (100.0±13.0 *vs.* 99.4±12.9%; U=15.0; n.s.; Fig. 6*D*).

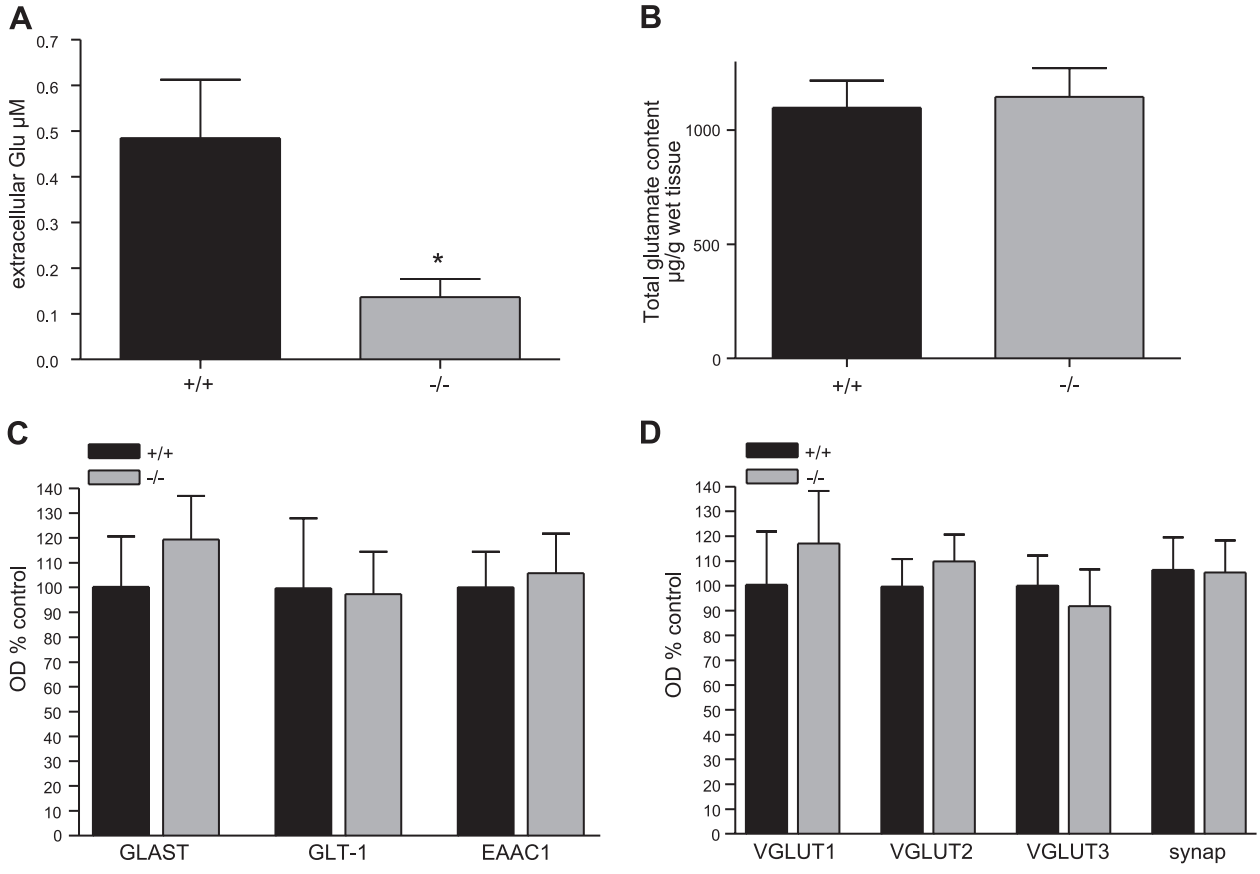

Figure 6. *A*) Extracellular glutamate concentrations (μM), as measured using *in vivo* microdialysis, in striatum of $xCT^{+/+}$ (n=7) and $xCT^{-/-}$ mice (n=8). *B*) Total striatal glutamate content (μg/g wet tissue), as measured in brain homogenates, in $xCT^{+/+}$ (n=6) and $xCT^{-/-}$ mice (n=6). *C, D*) Striatal protein expression levels of GLAST, GLT-1 and EAAC1 (*C*) and VGLUT1–3 and synaptophysin (*D*) in $xCT^{-/-}$ mice (n=6) relative to $xCT^{+/+}$ mice (n=6). Bars represent relative optical density as measured from a Western blotting experiment, normalized to GAPDH. *$P < 0.05$; Mann-Whitney U test.

Increase in cystine uptake and intracellular glutathione in C6 glioma in the presence of 6-OHDA

Adding 6-OHDA to C6 glioma in culture resulted in a dose-dependent significant increase in cystine uptake (nmol/min/mg protein; control: 0.330±0.006; 6-OHDA: 10 μM, 0.455±0.014; 20 μM, 0.597±0.013; 50 μM, 0.548±0.015; 1-way ANOVA with Bonferroni's *post hoc* test, $F_{3,20}$=85.92, P<0.0001; **Fig. 7*A***) as well as intracellular glutathione levels (nmol/mg protein; control: 48.92±1.64; 6-OHDA: 10 μM, 64.53±3.24; 20 μM, 71.74±3.08; 50 μM, 81.05±2.47; 1-way ANOVA with Bonferroni's *post hoc* test, $F_{3,20}$=25.55, P<0.0001; Fig. 7*B*). To confirm that the 6-OHDA-induced increase in cystine uptake is accomplished *via* an increase in activity of system x_c^- rather than a Na^+/K^+-dependent glutamate transporter, we measured cystine uptake in the cells treated with 6-OHDA in the presence and absence of Na^+. Although replacing Na^+ by choline decreased the basal (*i.e.*, without 6-OHDA treatment) cystine uptake (Na^+ *vs.* Na^+-free: 0.295±0.010 *vs.* 0.133±0.005 nmol/min/mg protein; 2-way ANOVA with Bonferroni's *post hoc* test, P<0.001, t=12.65), Na^+-independent activity of cystine uptake was induced by 6-OHDA treatment (basal *vs.* 6-OHDA treatment: 0.133±0.005 *vs.* 0.361±0.003 nmol/min/mg protein; 2-way ANOVA with Bonferroni's *post hoc* test, P<0.001, t=17.8; Fig. 7*C*). Substrates for system x_c^-, glutamate and HoA, inhibited the Na^+-independent activity of cystine uptake (nmol/min/mg protein; +glutamate: 0.024±0.003; +HoA: 0.017±0.004; 2-way ANOVA with Bonferroni's *post hoc* test, $F_{3,39}$=792.2, P<0.001), indicating that the Na^+-independent activity of cystine uptake induced by 6-OHDA treatment represents increased system x_c^- activity (Fig. 7*C*). Moreover, the significant increase in intracellular glutathione content caused by 6-OHDA treatment (control *vs.* 6-OHDA: 43.79±1.72

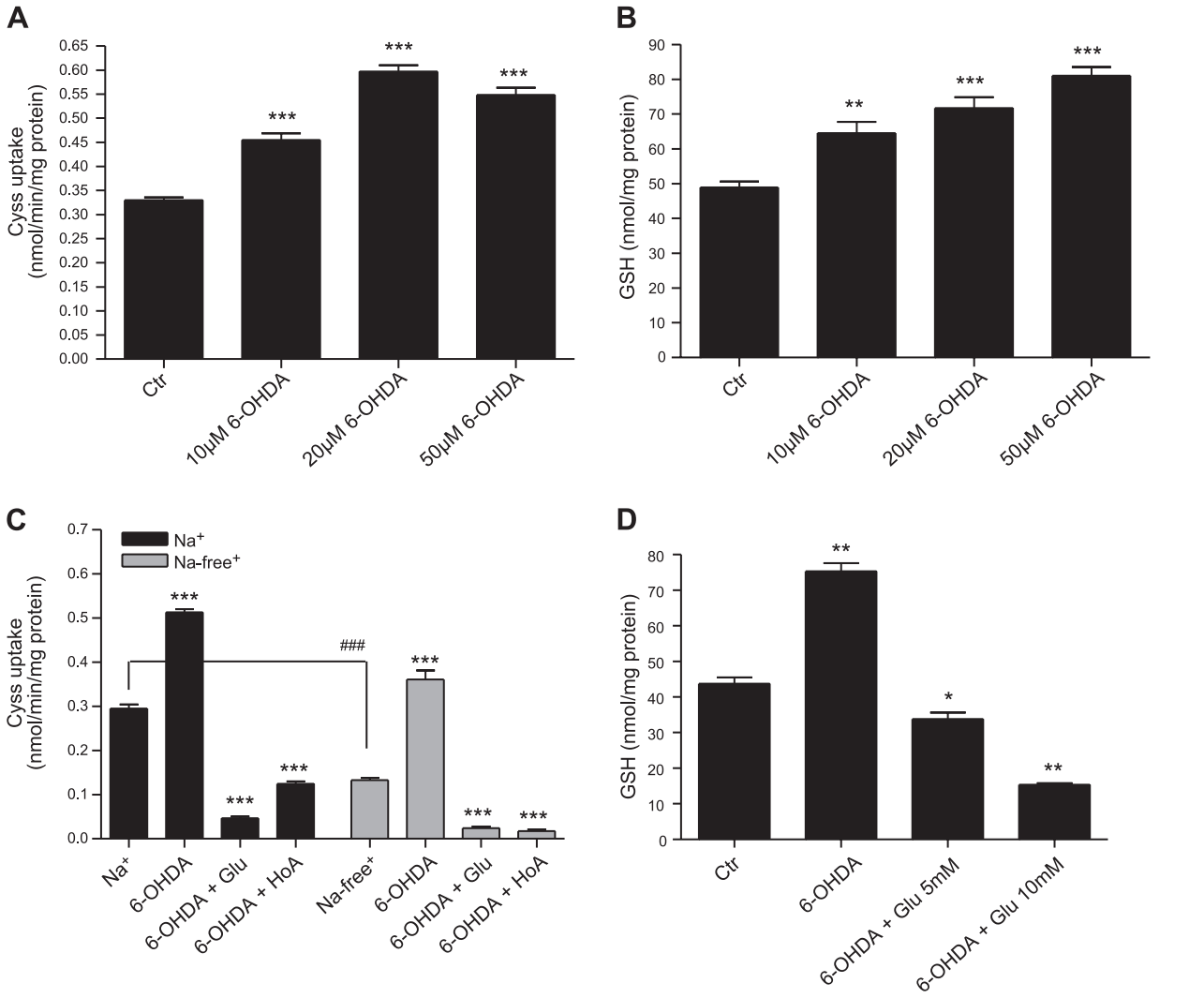

Figure 7. *A*, *B*) Cystine (Cyss; *A*) uptake and intracellular glutathione (GSH; *B*) levels in C6 glioma after 6-OHDA treatment (n=6/condition). *C*) Replacing Na^+ by choline in the uptake solution did not affect the 6-OHDA-induced increase in cystine uptake, whereas the addition of glutamate or HoA abolished and even reversed the 6-OHDA-induced increase in cystine uptake. *D*) High concentrations of glutamate in the uptake solution abolished and reversed the 6-OHDA-induced increase in intracellular GSH content (n=6/condition). $^*P < 0.05$, $^{**}P < 0.01$, $^{***}P < 0.001$ *vs.* control; $^{\#\#\#}P < 0.001$; 1-way (*A*, *B*) or 2-way (*C*, *D*) ANOVA followed by Bonferroni's *post hoc* test.

vs. 75.35±2.29 nmol/mg protein) was abolished and even reversed by culturing the cells with excess amounts of glutamate in a dose-dependent manner (nmol/mg protein; glutamate: 5 mM, 33.81±1.85; 10 mM, 15.37±0.42; 1-way ANOVA with Bonferroni's *post hoc* test, $F_{3,37}=158.7$, $P<0.001$; Fig. 7*D*).

DISCUSSION

In the present study, we identify system x_c^- as the main source of striatal extracellular glutamate in mice. Mice lacking functional system x_c^- do not show decreased glutathione content or any signs of increased oxidative stress. Yet, loss of glutamate release *via* system x_c^- protects neurons against 6-OHDA-induced toxicity, making system x_c^- a plausible target for the development of neuroprotective strategies for PD treatment.

Because of the prominent role of oxidative stress in PD pathogenesis and evidence for glutathione shortage in substantia nigra preceding neurodegeneration (2), we hypothesized that mice lacking functional system x_c^- (12) may be more sensitive to 6-OHDA-induced neurodegeneration. After all, by providing cystine to cells, system x_c^- has been shown to be an important regulator of intracellular glutathione levels and antioxidant capacity of the brain (3, 20). In view of this hypothesis, we speculated that the increased expression of xCT protein in the ipsilateral striatum of the hemi-Parkinson rat (9) might be an attempt of the brain to compensate for the 6-OHDA-induced increase in oxidative stress. Moreover, loss of Nrf2, a transcription factor that induces xCT expression, exacerbates vulnerability to the neurotoxin 6-OHDA (21). Also, mice with an overexpression of glutathione peroxidase or superoxide dismutase show attenuated 6-OHDA-induced neurotoxicity (22, 23).

In the present study, we show that striatal glutathione levels are unaltered in system x_c^--deficient mice, in line with an earlier observation of Chung *et al.* (24), who reported that nonmalignant cells, contrary to tumor cells, were not exclusively dependent on system x_c^- for cystine uptake. Moreover, $xCT^{-/-}$ mice did not show any signs of increased oxidative stress.

Also, the nigrostriatal dopaminergic pathway seemed unaffected in the $xCT^{-/-}$ mice. No difference was observed in striatal DA content, striatal DOPAC/DA ratio, or number of TH^+ profiles in the SNc of $xCT^{-/-}$ mice compared to wild-type littermates.

To investigate the sensitivity of $xCT^{-/-}$ mice for PD-inducing toxins, we examined brains for their striatal DA content and number of TH^+ profiles in the SNc at 3 and 10 d after striatal 6-OHDA injection. In sharp contrast to expectations, if the role of system x_c^- were cystine uptake for neuroprotection, dopaminergic neurons of 3-mo-old mice lacking functional system x_c^- are protected against 6-OHDA-induced neurodegeneration. Whereas the loss of striatal DA after 6-OHDA lesioning was equal between $xCT^{-/-}$ and $xCT^{+/+}$ mice, $xCT^{+/+}$ mice showed a significant loss of dopaminergic neurons in the SNc after toxin injection, contrary to $xCT^{-/-}$ mice. Because it was reported by Sato *et al.* (12) that plasma of $xCT^{-/-}$ mice is in a more oxidative state, possibly implying accelerated aging, we next investigated the vulnerability to 6-OHDA of 12- to 18-mo-old $xCT^{-/-}$ mice. Yet, also the aged $xCT^{-/-}$ mice were devoid of neurodegeneration, whereas wild-type littermates clearly showed neuronal loss. These data do not support the idea of accelerated aging, at least not in the brain. This correlates with our current and previous observations of comparable cortical thinning, comparable decrease in glutathione, and increase in number of $GFAP^+$ cells with age in hippocampus (unpublished results) and striatum of both genotypes, indicating that the brain of the $xCT^{-/-}$ mice is damaged to the same extent by the process of aging.

Neuroprotection could result from compensatory antioxidant mechanisms. Because $xCT^{-/-}$ mice do not show decreased glutathione levels or signs of increased oxidative stress, there should be a compensatory up-regulation of another mechanism providing intracellular cysteine. One might expect increased expression of EAAC1, a neuronal glutamate reuptake transporter that also imports cysteine (25–28), though we did not detect an up-regulation of striatal EAAC1 expression. Possibly, trafficking of EAAC1 from the intracellular pool to the cell membrane is affected by xCT deletion, with increased cell surface expression of EAAC1 as a result. This might be masked when total EAAC1 expression levels are measured. Yet, EAAC1 trafficking is considered to be a mechanism associated with rapid changes in function, occurring without the delay associated with protein synthesis (29). In further experiments, screening of other cysteine transport systems, such as system alanine-serine-cysteine (ASC) or systems L or A (nonselective cysteine transporters; ref. 30), as well as enzymes related to glutathione regeneration, should be performed in tissue of $xCT^{-/-}$ mice to explain the absence of glutathione shortage.

Notably, besides providing intracellular cysteine for glutathione synthesis, system x_c^- has been reported to be the major source of extracellular glutamate in rat nucleus accumbens (4). Here, we show for the first time that extracellular glutamate levels are significantly decreased in striatum of $xCT^{-/-}$ mice, in accordance with our observation in hippocampus (unpublished results). A reduction of 70% in striatal extracellular glutamate could be observed as a result of a deletion of xCT. Total striatal glutamate levels, as well as plasma glutamate levels (12), were unaffected in $xCT^{-/-}$ mice. Our data strongly suggest that neuroprotection in the SNc of $xCT^{-/-}$ mice might be linked to the decreased glutamate release *via* system x_c^-. Accordingly, Savaskan *et al.* (31) showed that a diminished glutamate secretion from gliomas due to xCT silencing could be linked to neuroprotection. Moreover, in *Drosophila melanogaster*, a shortened life span, as well as neurodegeneration, was observed as a result of overexpression of Genderblind, an xCT protein (7).

The present data illustrate that $xCT^{-/-}$ mice are not

protected against the primary toxicity of 6-OHDA, since striatal DA loss, and thus probably death of the dopaminergic afferents, is equal between both genotypes. Therefore, $xCT^{-/-}$ mice seem to be protected against more upstream toxicity, possibly resulting from a dysregulation of neurotransmission in the nuclei of the basal ganglia. Decreased DA levels in striatum are accompanied by increased extracellular glutamate levels in parkinsonian rodents, possibly resulting from hyperactivity of corticostriatal afferents (10, 11). In $xCT^{-/-}$ mice, however, overactivity of corticostriatal afferents might lead to increased extracellular glutamate levels; although, because of the decreased basal striatal extracellular glutamate levels, they could still be below the excitotoxicity threshold. Moreover, glutamate released extrasynaptically will affect glutamatergic neurotransmission *via* stimulation of extrasynaptic metabotropic glutamate (mGlu) receptors (4). Antagonists of group I mGlu receptors (mGlu1 and mGlu5), which are omnipresent throughout the nuclei of the basal ganglia (32), have been shown to exert neuroprotective properties (33) and mice lacking mGlu5 have been shown to be less sensitive to MPTP toxicity (34). Therefore, the loss of activation of these receptors due to the loss of glutamate release *via* system x_c^- might result in neuroprotection in our mouse model for PD.

Overactivity of the STN, an important factor in PD pathogenesis, could contribute, *via* direct excitatory projection to the SNc, to progressive degeneration of the nigrostriatal pathway (35, 36). Yet, because of the small dimensions of these nuclei, we do not know whether extracellular glutamate concentrations in the STN and/or SNc are decreased as well in the $xCT^{-/-}$ mice. However, because the role of system x_c^- in determining extracellular glutamate levels is not exclusively confined to the striatum (unpublished results), we speculate that xCT deletion also results in decreased extracellular glutamate in other nuclei of the basal ganglia.

Thus, in wild-type mice, in response to 6-OHDA-induced oxidative stress, one would expect increased activity of system x_c^- and thus possibly excitotoxic levels of glutamate and/or overactivation of mGlu1/5. Indeed, in the 6-OHDA hemi-Parkinson rat, we observed increased striatal xCT expression (9), and the present *in vitro* experiments clearly demonstrate that 6-OHDA treatment of C6 glioma results in increased cystine uptake, mediated *via* system x_c^-. We speculate that $xCT^{-/-}$ mice will respond to this increased load of hydroxyl radicals with another antioxidant system, avoiding an increase in extracellular glutamate. Qin *et al.* (6) already postulated that in Alzheimer's disease the increased xCT expression in microglia surrounding amyloid-β plaques might enhance amyloid-β toxicity *via* increased glutamate release. Also, Lewerenz and Maher (37) did not exclude from *in vitro* experiments that, although the up-regulation of xCT in Alzheimer's disease might be an adaptive neuroprotective response, as a detrimental side effect, it might lead to accelerated neuronal loss. The same might happen in the pathogenesis of PD, where oxidative stress is known to be an important mediator.

In summary, we show for the first time that 70% of extracellular glutamate in mouse striatum derives from release *via* system x_c^-. A loss of functional system x_c^-, and thus loss of glutamate release *via* system x_c^-, results in significantly decreased striatal extracellular glutamate and is accompanied by significant neuroprotection of dopaminergic neurons in the SNc against 6-OHDA toxicity. The current findings emphasize the need for continuing the search for specific inhibitors of system x_c^-, which might represent interesting tools for the development of neuroprotective therapies for the treatment of PD and other pathologies involving oxidative stress and increased extracellular glutamate concentrations. FJ

This work was supported by grants of the Brussels Capital Region (Prospective Research for Brussels), Fonds voor Wetenschappelijk Onderzoek (FWO)-Flanders, and the Vrije Universiteit Brussel. A.S. is a research assistant of the FWO-Flanders and K.V. is a research assistant of the Agentschap voor Innovatie door Wetenschap en Technologie (IWT)-Flanders. The authors thank Mr. G. De Smet and Ms. A. De Smet for excellent technical assistance, as well as Dr. M. Watanabe (Hokkaido University Schoo1 of Medicine, Sapporo, Japan) for providing antibodies.

REFERENCES

1. Blandini, F., Nappi, G., Tassorelli, C., and Martignoni, E. (2000) Functional changes in the basal ganglia circuitry in Parkinson's disease. *Prog. Neurobiol.* **62,** 63–88
2. Schulz, J. B., Lindenau, J., Seyfried, J., and Dichgans, J. (2000) Glutathione, oxidative stress and neurodegeneration. *Eur. J. Biochem.* **267,** 4904–4911
3. Bannai, S. (1986) Exchange of cystine and glutamate across plasma membrane of human fibroblasts. *J. Biol. Chem.* **261,** 2256–2263
4. Baker, D. A., Xi, Z.-X., Shen, H., Swanson, C. J., and Kalivas, P. (2002) The origin and neuronal function of in vivo nonsynaptic glutamate. *J. Neurosci.* **22,** 9134–9141
5. Sontheimer, H. (2003) Malignant gliomas: perverting glutamate and ion homeostasis for selective advantage. *Trends Neurosci.* **26,** 543–549
6. Qin, S., Colin, C., Hinners, I., Gervais, A., Cheret, C., and Mallat, M. (2006) System x_c^- and apolipoprotein E expressed by microglia have opposite effects on the neurotoxicity of amyloid-β peptide 1–40. *J. Neurosci.* **26,** 3345–3356
7. Augustin, H., Grosjean, Y., Chen, K., Sheng, Q., and Featherstone, D. E. (2007) Nonvesicular release of glutamate by glial xCT transporters suppresses glutamate receptor clustering in vivo. *J. Neurosci.* **27,** 111–123
8. Albrecht, P., Lewerenz, J., Dittmer, S., Noack, R., Maher, P., and Methner, A. (2010) Mechanisms of oxidative glutamate toxicity: the glutamate/cystine antiporter system x_c^- as a neuroprotective drug target. *CNS Neurol. Disord. Drug Targets* **9,** 373–382
9. Massie, A., Schallier, A., Mertens, B., Vermoesen, K., Bannai, S., Sato, H., Smolders, I., and Michotte, Y. (2008) Time-dependent changes in striatal xCT protein expression in hemi-Parkinson rats. *NeuroReport* **19,** 1589–1592
10. Lindefors, N., and Ungerstedt, U. (1990) Bilateral regulation of glutamate tissue and extracellular levels in caudate-putamen by midbrain dopamine neurons. *Neurosci. Lett.* **115,** 248–252
11. Meshul, C. K., Emre, N., Nakamura, C. M., Allen, C., Donohue, M. K., and Buckman, J. F. (1999) Time-dependent changes in striatal glutamate synapses following a 6-hydroxydopamine lesion. *Neuroscience* **88,** 1–16

12. Sato, H., Shiiya, A., Kimata, M., Maebara, K., Tamba, M., Sakakura, Y., Makino, N., Sugiyama, F., Yagami, K., Moriguchi, T., Takahashi, S., and Bannai, S. (2005) Redox imbalance in cystine/glutamate transporter-deficient mice. *J. Biol. Chem.* **280,** 37423–37429
13. Paxinos, G., and Franklin, K. B. J. (2007) *The Mouse Brain in Stereotaxic Coordinates, 3rd Ed.*, Academic Press, San Diego, CA, USA
14. Shu, S., Ju, G., and Fan, L. (1988) The glucose oxidase-DAB-nickel method in peroxidase histochemistry of the nervous system. *Neurosci. Lett.* **84,** 169–171
15. Coggeshall, R. E., and Lekan, H. A. (1996) Methods for determining numbers of cells and synapses: a case for more uniform standards of review. *J. Comp. Neurol.* **364,** 6–15
16. Massie, A., Schallier, A., Vermoesen, K., Arckens, L., and Michotte, Y. (2010) Biphasic and bilateral changes in striatal VGLUT1 and 2 protein expression in hemi-Parkinson rats. *Neurochem. Int.* **57,** 111–118
17. Yamada, K., Watanabe, M., Shibata, T., Nagashima, M., Tanaka, K., and Inoue, Y. (1998) Glutamate transporter GLT-1 is transiently localized on growing axons of the mouse spinal cord before establishing astrocytic expression. *J. Neurosci.* **18,** 5706–5713
18. Shibata, T., Yamada, K., Watanabe, M., Ikenaka, K., Wada, K., Tanaka, K., and Inoue, Y. (1997) Glutamate transporter GLAST is expressed in the radial glia-astrocyte lineage of developing mouse spinal cord. *J. Neurosci.* **17,** 9212–9219
19. Van Hemelrijck, A., Sarre, S., Smolders, I., and Michotte, Y. (2005) Determination of amino acids associated with cerebral ischaemia in rat brain microdialysates using narrowbore liquid chromatography and fluorescence detection. *J. Neurosci. Methods* **144,** 63–71
20. Mandal, P. K., Seiler, A., Perisic, T., Kölle, P., Canak, A. B., Förster, H., Weiss, N., Kremmer, E., Lieberman, M. W., Bannai, S., Kuhlencordt, P., Sato, H., Bornkamm, G. W., and Conrad, M. (2010) System x_c^- and thioredoxin reductase 1 cooperatively rescue glutathione deficiency. *J. Biol. Chem.* **285,** 22244–22253
21. Jakel, R. J., Townsend, J. A., Kraft, A. D., and Johnson, J. A. (2007) Nrf2-mediated protection against 6-hydroxydopamine. *Brain Res.* **1144,** 192–201
22. Bensadoun, J. C., Mirochnitchenko, O., Inouye, M., Aebischer, P., and Zurn, A. D. (1998) Attenuation of 6-OHDA-induced neurotoxicity in glutathione peroxidase transgenic mice. *Eur. J. Neurosci.* **10,** 3231–3236
23. Asanuma, M., Hirata, H., and Cadet, J. L. (1998) Attenuation of 6-hydroxydopamine-induced dopaminergic nigrostriatal lesions in superoxide dismutase transgenic mice. *Neuroscience* **85,** 907–917
24. Chung, W. J., Lyons, S. A., Nelson, G. M., Hamza, H., Gladson, C. L., Gillespie, G. Y., and Sontheimer, H. (2005) Inhibition of cystine uptake disrupts the growth of primary brain tumors. *J. Neurosci.* **25,** 7101–7110
25. Shanker, G., Allen, J. W., Mutkus, L. A., and Aschner, M. (2001) The uptake of cysteine in cultured primary astrocytes and neurons. *Brain Res.* **902,** 156–163
26. Chen, Y., and Swanson, R. A. (2003) The glutamate transporters EAAT2 and EAAT3 mediate cysteine uptake in cortical neuron cultures. *J. Neurochem.* **84,** 1332–1339
27. Himi, T., Ikeda, M., Yasuhara, T., Nishida, M., and Morita, I. (2003) Role of neuronal glutamate transporter in the cysteine uptake and intracellular glutathione levels in cultured cortical neurons. *J. Neural Transm.* **110,** 1337–1348
28. Aoyama, K., Suh, S. W., Hamby, A. M., Liu, J., Chan, W. Y., Chen, Y., and Swanson, R. A. (2006) Neuronal glutathione deficiency and age-dependent neurodegeneration in the EAAC1 deficient mice. *Nat. Neurosci.* **9,** 119–126
29. Fournier, K. M., Gonzalez, M. I., and Robinson, M. B. (2004) Rapid trafficking of the neuronal glutamate transporter, EAAC1: evidence for distinct trafficking pathways differentially regulated by protein kinase C and platelet-derived growth factor. *J. Biol. Chem.* **279,** 34505–34513
30. Christensen, H. N. (1990) Role of amino acid transport and countertransport in nutrition and metabolism. *Physiol. Rev.* **70,** 43–77
31. Savaskan, N. E., Heckel, A., Hahnen, E., Engelhorn, T., Doerfler, A., Ganslandt, O., Nimsky, C., Buchfelder, M., and Eyüpoglu, I. Y. (2008) Small interfering RNA-mediated xCT silencing in gliomas inhibits neurodegeneration and alleviates brain edema. *Nat. Med.* **14,** 629–632
32. Rouse, S. T., Marino, M. J., Bradley, S. R., Awad, H., Wittmann, M., and Conn, P. J. (2000) Distribution and roles of metabotropic glutamate receptors in the basal ganglia motor circuit: implications for treatment of Parkinson's disease and related disorders. *Pharmacol. Ther.* **88,** 427–435
33. Vernon, A. C., Zbarsky, V., Datla, K. P., Croucher, M. J., and Dexter, D. T. (2007) Subtype selective antagonism of substantia nigra pars compacta group I metabotropic glutamate receptors protects the nigrostriatal system against 6-hydroxydopamine toxicity in vivo. *J. Neurosci.* **103,** 1075–1091
34. Battaglia, G., Busceti, C. L., Molinaro, G., Biagioni, F., Storto, M., Fornai, F., Nicoletti, F., and Bruno, V. (2004) Endogenous activation of mGlu5 metabotropic glutamate receptors contributes to the development of nigro-striatal damage by 1-methyl-1,2,3,6-tetrahydropyridine in mice. *J. Neurosci.* **24,** 828–835
35. Rodriguez, M. C., Obeso, J. A., and Olanow, C. W. (1998) Subthalamic nucleus-mediated excitotoxicity in Parkinson's disease: a target for neuroprotection. *Ann. Neurol.* **44,** S175–S188
36. Blandini, F. (2001) The role of the subthalamic nucleus in the pathophysiology of Parkinson's disease. *Funct. Neurol.* **164,** 99–106
37. Lewerenz, J., and Maher, P. (2009) Basal levels of eIF2α phosphorylation determine cellular antioxidant status by regulating ATF4 and xCT expression. *J. Biol. Chem.* **284,** 1106–1115

Received for publication November 30, 2010.
Accepted for publication December 16, 2010.